Redox Biology 19 (2018) 190–199

Contents lists available at ScienceDirect

Redox Biology

journal homepage: www.elsevier.com/locate/redox

Research Paper

Suppression of hERG K^+ current and cardiac action potential prolongation by 4-hydroxynonenal via dual mechanisms

Seong Woo Choi[a,b], Si Won Choi[a], Young Keul Jeon[a], Sung-Hwan Moon[b], Yin-Hua Zhang[a], Sung Joon Kim[a,*]

[a] Department of Physiology, Seoul National University College of Medicine, Seoul, Republic of Korea
[b] Department of Stem Cell Biology, Konkuk University School of Medicine, Seoul, Republic of Korea

ARTICLE INFO

Keywords:
Lipid peroxidant
4-hydroxynonenal
hERG channel
Cardiac action potential prolongation

ABSTRACT

Oxidative stress under pathological conditions, such as ischemia/reperfusion and inflammation, results in the production of various reactive chemicals. Of these chemicals, 4-hydroxynonenal (4-HNE), a peroxidation product of ω6-polyunsaturated fatty acid, has garnered significant attention. However, the effect of 4-HNE on cardiac electrophysiology has not yet been reported. In the present study, we investigated the effects of 4-HNE on several cardiac ion channels, including human ether-a-go-go-related (hERG) channels, using the whole-cell patch clamp technique. Short-term exposure to 100 μM 4-HNE (4-HNE_{100S}), which mimics local levels under oxidative stress, decreased the amplitudes of rapidly activating delayed rectifier K^+ current (I_{Kr}) in guinea pig ventricular myocytes (GPVMs) and HEK293T cells overexpressing hERG (I_{hERG}). MS analysis revealed the formation of 4-HNE-hERG adduct on specific amino acid residues, including C276, K595, H70, and H687. Long-term treatment (1–3 h) with 10 μM 4-HNE (4-HNE_{10L}), suppressed I_{Kr} and I_{hERG}, but not I_{Ks} and $I_{Ca,L}$. Action potential duration (APD) of GPVMs was prolonged by 37% and 64% by 4-HNE_{100S} and 4-HNE_{10L}, respectively. Western blot analysis using surface biotinylation revealed a reduction in mature membrane hERG protein after treatment with 4-HNE_{10L}. Proteasomal degradation inhibitors, such as bortezomib, prevented the 4-HNE_{10L}-induced decrease in mature hERG, suggesting a retrograde degradation of membrane hERG due to 4-HNE. Taken together, 4-HNE_{100S} and 4-HNE_{10L} suppressed I_{hERG} via functional inhibition and downregulation of membrane expression of hERG, respectively. The exposure of 4-HNE under pathological oxidative stress may increase the risk of proarrhythmic events via APD prolongation.

1. Introduction

Human *ether-a-go-go*-related gene (*KCNH2*) encodes hERG protein (Kv11.1), which is responsible for the rapidly activating delayed rectifier potassium current (I_{Kr}) in cardiomyocytes. I_{Kr} is critical for determining the cardiac action potential duration (APD) and QT interval in electrocardiograms [1]. Functional impairment of I_{Kr} due to genetic mutations in hERG or exposure to various cardiotoxic drugs can induce inherited or acquired long QT syndrome (LQTS), respectively [2]. It has been suggested that dysregulation of hERG channels by excessive reactive oxygen species production under oxidative stress increases the risk of arrhythmia [3–5]. A recent study demonstrated that application of hydrogen peroxide (H_2O_2) decreases the hERG current (I_{hERG}) by directly interacting with Cys^{723} in the cytoplasmic C-terminal [6]. However, it is not known whether alternative intrinsic oxidative agents, such as lipid peroxidants, affect hERG via a similar mechanism, especially during the long-term exposure.

The compound 4-hydroxynonenal (4-HNE) is a highly reactive end-product of polyunsaturated fatty acid oxidation that forms protein adducts with nucleophilic residues, such as cysteine, histidine and lysine. Under physiological conditions, 4-HNE is conjugated to glutathione, or metabolized by aldehyde reductase and aldehyde dehydrogenase [7,8]. However, under conditions of severe oxidative stress with decreased metabolization, 4-HNE accumulates and becomes a significant pathophysiolgical factor [9,10] and can act as a toxic mediator of free radicals [11]. The physiological concentrations of 4-HNE in interstitial

Abbreviations: I_{Kr}, rapidly activating delayed rectifier potassium current in cardiomyocyte; I_{Ks}, slowly activating delayed rectifier potassium current in cardiomyocyte; $I_{Ca,L}$, , L-type calcium current in cardiomyocyte; I_{hERG}, outward K^+ current in hERG overexpressed conditions; APD, action potential duration; V_{max}, maximal upstroke velocity; RMP, resting membrane potential; TA, total amplitude; LQTS, long QT syndrome; GPVM, guinea pig ventricular myocyte

* Correspondence to: Department of Physiology, Seoul National University College of Medicine, 103 Daehak-ro, Jongro-gu, Seoul, Republic of Korea.
E-mail address: sjoonkim@snu.ac.kr (S.J. Kim).

https://doi.org/10.1016/j.redox.2018.08.018
Received 2 August 2018; Received in revised form 20 August 2018; Accepted 23 August 2018
Available online 24 August 2018

fluids range from 0.3 to 5 μM and increase by 10–100 fold under pathological conditions [12,13]. Although 4-HNE concentrations are lower in plasma than in tissues, elevated plasma 4-HNE concentrations (1–10 μM) have been observed in patients experiencing ischemic brain hemorrhage and stroke [14,15].

Previous studies have suggested pathophysiological roles of 4-HNE accumulation in cardiovascular diseases, such as ischemia-reperfusion injury, dilated heart dysfunction, heart failure, and atherosclerosis [16–19]. However, the influence of 4-HNE on cardiac ion channels and action potential (AP) is poorly understood. An early study of rat ventricular myocytes demonstrated that a treatment with 400 μM of 4-HNE increased APD, depolarized the resting membrane potential (RMP), increased the window current of Na^+ channels, and decreased the inward rectifier K^+ current [20]. However, it is not known whether 4-HNE regulates I_{Kr} and I_{Ks} (slowly activating delayed rectifier potassium current), which are essential for determining APD and are frequently intrinsic to pharmacological arrhythmogenesis. Moreover, the effects of physiologically or pathophygiolgically meaningful concentrations (5–100 μM) of 4-HNE on the cardiac ion channels have yet to be characterized. Considering that the relatively lower concentration (ca. 10 μM) of 4-HNE can be maintained in plasma for a prolonged period in the brain hemorrhage and stroke [14,15], it is requested to examine the effects of both short- and long-term effects on the cardiac ion channels.

On these backgrounds, we investigated the effect of short-term (< 10 min) and long-term (0.5–12 h) 4-HNE exposure on cardiac ion channels and APD in primary guinea pig ventricular myocytes (GPVMs) and HEK293 cells overexpressing hERG. To clarify the adduct formation between hERG and 4-HNE, mass spectrometry post-translational modification (PTM) analysis was performed. Furthermore, membrane expression of the mature form of hERG was measured to characterize the effects of long-term exposure to 4-HNE on the lifetime of functional hERG.

2. Methods and materials

2.1. Cell culture and plasmid transfection

Basic electrophysiological studies of I_{hERG} and hERG protein expression were performed using HEK293 cells stably expressing hERG1a (hERG-HEK cells) kindly donated by Dr. Han Choe (University of Ulsan, Seoul, Korea). The hERG-HEK cells were maintained in minimum essential medium (Gibco, Carlsbad, CA, USA) supplemented with 10% fetal bovine serum (Serana Europe, Pessin, Germany). For electrophysiological studies using transient expression systems, human isoform of KCNH2 (hERG1a), KCNQ1, and KCNE1 channels were used. Except for wild-type hERG1a (hERG-HEK cells), all complementary DNA was transiently transfected into HEK293 cells using FuGENE 6 kit (Roche, Penzberg, Germany). Detailed cell culture and transfection methods have been published previously [21].

2.2. Isolation of GPVMs

Male guinea pigs (weighing ~ 350 g) were purchased from Koatech (Seoul, Korea). The guinea pigs were housed in standard cages and light conditions and fed a standard diet with ad libitum access to drinking water. All animal experiments were approved by the Institutional Animal Care and Use Committee of Seoul National University (Approval number: SNU-141125-3-1). Guinea-pigs were anesthetized using an intraperitoneal injection of a mixture of pentobarbital sodium (50 mg/kg) and heparin (300 U/ml). The heart was transferred to a Langendorff apparatus and then retrogradely perfused with Ca^{2+}-free Tyrode's solution (135 mM NaCl, 5.4 mM KCl, 3.5 mM $MgCl_2$, 5 mM glucose, 5 mM HEPES, 0.4 mM Na_2HPO_4, and 20 mM taurine adjusted to a pH 7.4 using NaOH) containing collagenase (1 mg/ml, Worthington Biochemical Co., NJ, USA), protease (0.1 mg/ml, Sigma), and 1% bovine serum albumin (Sigma, St. Louis, MO, USA). After 10 min of enzyme perfusion, the left ventricle was isolated and digested again with fresh collagenase-containing Tyrode's solution for 8 min. Isolated GPVMs were kept in Kraft-Bruhe (K-B) solution (70 mM KOH, 55 mM KCl, 20 mM KH_2PO_4, 10 mM HEPES, 20 mM glucose, 50 mM L-glutamate, 20 mM taurine, 0.5 mM EGTA, and 3 mM $MgCl_2$ adjusted to a pH 7.3 with KOH) at 4 °C.

2.3. Electrophysiological recording

Conventional whole-cell voltage and current clamps were performed at room temperature. The signals were amplified and digitized with an Axopatch 200B amplifier (Axon Instruments, Foster, CA, USA) and Digidata 1440B AD-DA converter (Axon Instruments). For electrophysiological recording and analysis of currents and AP, pClamp 10.1 (Axon Instruments) and Origin 8.0 (Microcal, Northampton, MA, USA) were used. Microglass pipettes (World Precision Instruments, Sarasota, FL, USA) were pulled to resistances of 2–3 MΩ with a PP-830 puller (Narishige, Tokyo, Japan). A 3 M KCl agar bridge was used to prevent junction potential artifacts when reducing agents were used [22]. I_{Kr} was recorded in either hERG-HEK cells or GPVMs. I_{Ks} was recorded in either HEK293 cells transiently transfected with KCNQ1/KCNE1 (KCNQ1/E1-HEK cells) or GPVMs. $I_{Ca,L}$ and AP were recorded in GPVMs.

The extracellular bath solution for I_{Kr} and I_{Ks} recordings in hERG-HEK cells contained 145 mM NaCl, 3.6 mM KCl, 10 mM HEPES, 1 mM $MgCl_2$, 1.3 mM $CaCl_2$, and 5 mM glucose adjusted to a pH 7.4 with NaOH. The intracellular pipette solution for I_{Kr} and I_{Ks} recording contained 100 mM K-aspartate, 25 mM KCl, 5 mM NaCl, 10 mM HEPES, 1 mM $MgCl_2$, 4 mM MgATP, and 10 mM BAPTA adjusted to pH 7.25 with KOH. Extracellular bath solution for recording I_{Kr} and I_{Ks} from GPVMs contained 145 mM NaCl, 5.4 mM KCl, 10 mM HEPES, 1 mM $MgCl_2$, 1.8 mM $CaCl_2$, 5 mM glucose, and 0.001 mM nifedipine adjusted to pH 7.4 with NaOH. I_{Kr} and I_{Ks} from GPVMs were isolated using the selective inhibitors E4031 (1 μM) and chromanol293B (Ch293B; 10 μM), respectively. The intracellular solution contained 120 mM K-aspartate, 20 mM KCl, 5 mM NaCl, 2 mM $CaCl_2$, 5 mM EGTA, 10 mM HEPES, and 5 mM MgATP adjusted to pH 7.25 with KOH. The compositions of the extracellular and intracellular solutions used for AP recording were same as for the I_{Kr} and I_{Ks} recording solutions except for the absence of nifedipine. The extracellular bath solution for $I_{Ca,L}$ contained 145 mM CsCl, 10 mM HEPES, 1 mM $MgCl_2$, 1.8 mM $CaCl_2$, and 5 mM glucose adjusted to pH 7.4 with CsOH. The intracellular solution for $I_{Ca,L}$ contained 106 mM CsCl, 20 mM TEA-Cl, 5 mM NaCl, 10 mM HEPES, 5 mM MgATP, and 10 mM EGTA adjusted to pH 7.25 with CsOH.

2.4. Surface biotinylation and Western blot analysis

For surface biotinylation, 4-HNE-treated hERG-HEK cells were washed twice with ice-cold PBS and then incubated with PBS containing 1 mg/ml of Sulfo-NHE-SS-Biotin (Thermo Fisher Scientific, Waltham, MA, USA) for 1 h at 4 °C. Cells were then incubated with 50 mM tris (pH 7.4) for 20 min at 4 °C to quench unreacted biotin. Following cell lysis, biotinylated proteins were recovered by incubating the cell lysates with NeutrAvidin-coated agarose Beads (Thermo Fisher Scientific) in PBS buffer for 1 h at room temperature. Beads were then washed 5 times with PBS plus 0.1% SDS. Biotinylated proteins were eluted from the beads in 2X Laemmli sample buffer + β-mercaptoethanol at 37 °C for 30 min. Eluted proteins were separated on 4–12% gradient gels (Koma Biotech, Seoul, Korea) and analyzed by Western blot.

Whole cell lysates from hERG-HEK cells were used for Western blot analysis. For mature (155 kDa) and immature (135 kDa) hERG detection, proteins were separated on 6% tris-glycine gels and electroblotted on polyvinylidene difluoride membranes. The membranes were immunoblotted with a rabbit anti-KCNH2 primary antibody (ab81160, Abcam, Cambridge, UK). Detection of hERG signals was performed

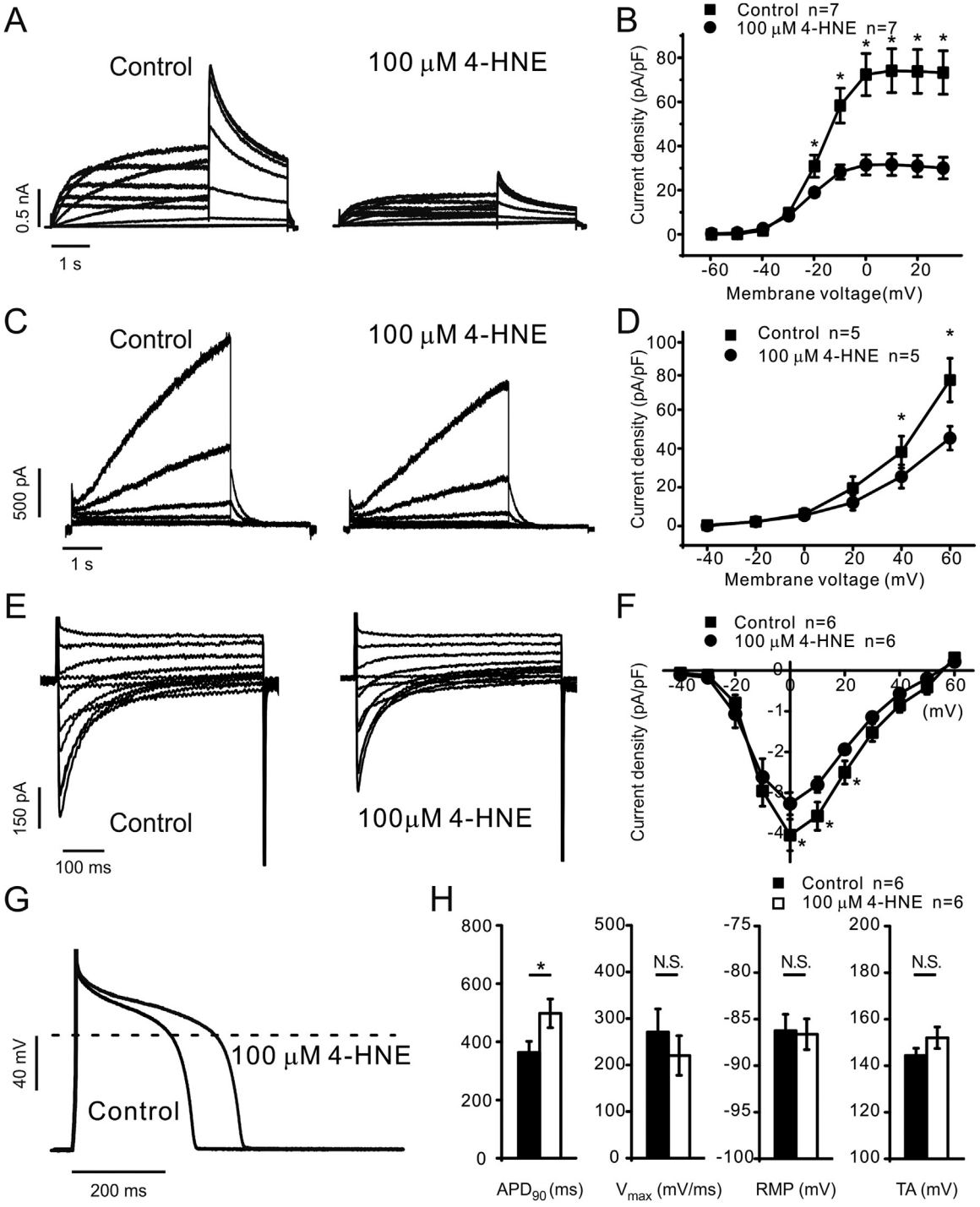

Fig. 1. Effects of 4-HNE_{100S} on delayed rectifier potassium currents, L-type calcium currents and action potential. (A and B) In hERG-HEK cells, rapidly activating delayed rectifier potassium currents (I_{Kr}) were activated by incremental depolarizing steps and common return voltage (− 40 mV). Summary of the peak outward tail current densities (pA/pF) according to test pulses (B) indicate that the I_{Kr} amplitudes were significantly decreased by 4-HNE_{100S}. (C and D) In KCNQ1/KCNE1-transfected HEK cells, sustained depolarization revealed slowly activating delayed rectifier potassium current (I_{Ks}). The I-V curves of maximum outward currents showed inhibitory effect of 4-HNE_{100S}. (E and F) L-type calcium currents ($I_{Ca,L}$) were recorded in guinea pig ventricular myocytes (GPVMs), and the depolarizing voltage-induced inward currents were decreased by 4-HNE_{100S}. (G and H) Action potentials (APs) were recorded in GPVMs under zero-current clamp mode. Total amplitudes (TA), resting membrane potential (RMP), and maximal upstroke velocity (V_{max}) were not affected, whereas the AP duration (APD_{90}) was prolonged by 4-HNE_{100S}. All the data were analyzed using paired *t*-tests, where a $P < 0.05$ was considered statistically significant.

using goat anti-rabbit secondary antibody and an ECL detection kit (Amersham Bioscience, Little Chalfont, UK).

2.5. Drugs for electrophysiology and protein degradation study

The compound 4-HNE was purchased from Cayman Chemical (MI, USA) as stock solution of 10 mg/ml in ethanol and store in − 80 °C. Immediately prior to the application, 4-HNE was freshly diluted with

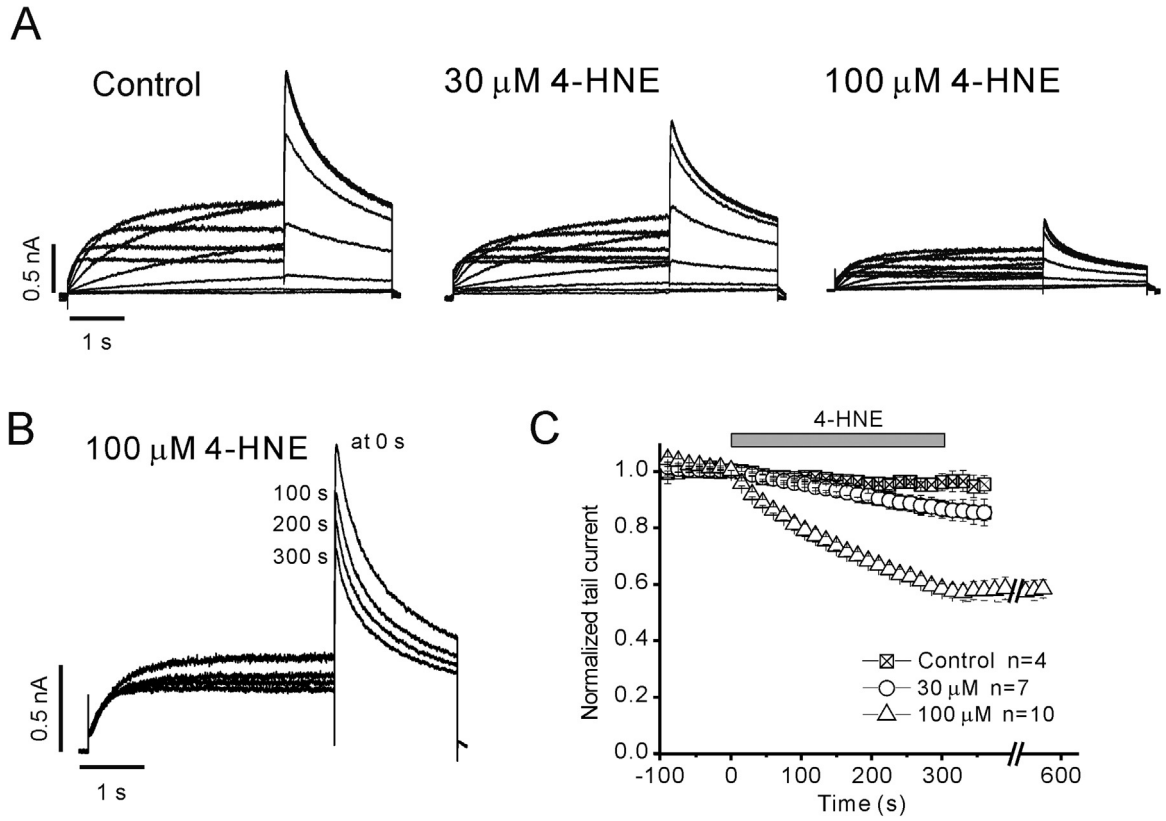

Fig. 2. Concentration-dependent inhibition of I_{Kr} by 4-HNE. (A) Representative traces of I_{Kr} in hERG-HEK cells treated with 30 and 100 μM 4-HNE for 300 s (B) Overlaid traces of single test pulse-induced I_{Kr} (40 mV) at different times of exposure to 100 μM 4-HNE. (C) Summarized plotting of peak tail currents normalized to the initial level in each cell. I_{Kr} amplitudes were gradually decreased under 4-HNE for 300 s, and the reduced currents were not reversible up to 300 s of washout.

extracellular solution to the final target concentrations. Tris(2-carboxyethyl)phosphine (TCEP), bafilomycin, E4031, Ch293B, and nifedipine were purchased from Sigma Chemicals (St. Louis, MO, USA). Bortezomib was purchased from Merck Millipore (Darmstadt, Germany).

2.6. Post-translational modification analysis

Whole cell lysates were subjected to SDS-PAGE. hERG bands were cut from the SDS-PAGE gel and digested in gel with trypsin (Promega, WI, USA). Tryptic digests of hERG are subsequently separated by online reversed-phase chromatography for each run using a Thermo Scientific Eazynano LC II autosampler with a reversed-phase peptide trap EASY-Column (100 μm inner diameter, 2 cm length) and a reversed-phase analytical EASY-Column (75 μm inner diameter, 10 cm length, 3 μm particle size, both Thermo Scientific), and electrospray ionization was subsequently performed using a 30 μm (i.d.) nano-bore stainless steel online emitter (Thermo Scientific) and a voltage set at 2.6 V, at a flow rate of 300 nl/min. The chromatography system was coupled on-line with an LTQ VelosOrbitrap mass spectrometer equipped with an ETD source. To improve peptide fragmentation of phosphopeptides, we applied a data dependent neutral loss MS3 ETD mode or a data dependent decision tree (DDDT) to select for collision induced dissociation (CID) or electron transfer dissociation (ETD) fragmentation depending from the charge sates, respectively. Protein identification was accomplished utilizing the Proteome Discoverer v1.3 database search engine (Thermo scientific) and searches were performed against IPI.human.v3.2 FASTA database or human MRS FASTA database. A fragment mass tolerance of 1.0 Da, peptide mass tolerance of 25 ppm, and maximum missed cleavage of 2 was set. Result filters were performed with peptide rank (Maximum rank: 1), peptides number per protein (Minimal number of peptides: 2, Count only rank 1 peptides: True, Count peptide only in top scored proteins: True) and Charge State versus Score (Score to which the filter is applied: Sequest Node (XCorr), Minimal Score for charge state = +1: 1.7, + 2: 2.5, + 3: 3.2, > + 4: 3.5). The Carbamidomethylation (+ 57.021 Da) of cysteine (C) is set as a Static Modification, and the following variable modification were allowed: Michael addition/+ 156.1 Da (C, K, H), Schiff base addition/ + 138.1 Da (K), Oxidation/+ 15.995 Da (M). Each processed data was subsequently transformed to.sf file with Scaffold 3 program and finally all PTMs identified from control or 4-HNE-treated sample, respectively were scored and compared with Scaffold PTM software.

2.7. Statistical analysis

For data analysis, Origin 8.0 and GraphPad Prism 6.0 software (GraphPad Software, La Jolla, CA, USA) were used. Data are presented as mean ± standard error of the mean. Statistical analyses were performed using paired or unpaired Student's *t*-tests. In all tests, a $P < 0.05$ was considered statistically significant.

3. Results

3.1. I_{hERG} decrease and APD increase by short-term exposure to 100 μM 4-HNE

First, we examined the effects of short-term exposure (300 s) to 100 μM 4-HNE (4-HNE_{100S}) on I_{Kr}, I_{Ks}, $I_{Ca,L}$, and cardiac AP. In this experiment, I_{Kr} and I_{Ks} were recorded in hERG- and KCNQ1/E1-HEK cells. $I_{Ca,L}$ and AP were recorded in GPVMs. To investigate the short-term effect, 100 μM of 4-HNE was applied through the bath perfusate after confirming the stable ionic currents. Treatment with 4-HNE_{100S} decreased the tail current amplitude of I_{Kr} to 41% of the control at − 40 mV return voltage (Fig. 1A and B; peak tail current after 30 mV of

activation voltage, 73.7 ± 9.96 and 30.9 ± 4.87 pA/pF for control and 4-HNE, respectively). I_{Ks} and $I_{Ca,L}$ were also reduced by 4-HNE_{100S} treatment but to a lesser extent (Fig. 1C–F; maximum I_{Ks} at 60 mV of activation voltage, 75.2 ± 11.23 and 45.3 ± 6.14 pA/pF and $I_{Ca,L}$ at 0 mV, − 4.0 ± 0.38 and − 3.2 ± 0.27 pA/pF for control and 4-HNE, respectively). Inhibition of I_{Ks} and $I_{Ca,L}$ was immediately reversed by washout of 4-HNE_{100S} (data not shown).

To record the AP in GPVMs under current clamp conditions, the myocytes were triggered by 1 Hz of current injection. 4-HNE_{100S} significantly increased the APD in an irreversible manner (Fig. 1G). The APD_{90} was prolonged from 359.3 ± 38.47–493.7 ± 49.33 ms; increase by about 37% when normalized to the untreated control. The maximal upstroke velocity (V_{max}), RMP, and total amplitude (TA) of the AP were not significantly altered (Fig. 1H).

The acute inhibition of I_{hERG} by 4-HNE was also observed at 30 μM while not at 10 μM (Fig. 2A). It was notable that the decrease in I_{hERG} was gradual, and did not reach a complete steady-state within the period of application (300 s, Fig. 2B and C). Moreover, the inhibitory effect of 4-HNE_{100S} on I_{hERG} was not spontaneously reversed by washout only up to 5 min (Fig. 2C, triangle).

3.2. 4-HNE adduct formation of hERG

After confirming the functional changes of hERG by 4-HNE treatment, tandem mass spectrometry was conducted to map the sites of PTM including 4-HNE adducts of hERG in hERG-HEK cells incubated with 100 μM 4-HNE for 10 min. 8 different sites of modification were localized by both SEQUEST and X! Tandem search engine (Table 1). Four of them were intrinsic modification sites of hERG (Table 1b. 4-HNE adduct on Cys^{1015}, Lys^{373}, Lys^{538}, and Lys^{748} identified in both 4-HNE-treated and untreated hERG). A representative MS/MS spectrum for the peptide ^{272}SRESCASCR^{280} shows that Cys^{276} is modified with a 4-HNE Michael adduct (Fig. 3A). Another spectrum shows the Schiff base adduct of Lys^{595} in the peptide ^{583}IGWLHNLGDQIGK^{595} (Fig. 3B). The spectrums of the peptide ^{63}PCTCDFLHGPR^{73} and ^{686}FHQIPNPLRQR^{696} revealed that His^{70} and His^{687} are modified with Michael adducts of 4-HNE, respectively (Fig. 3C and D).

3.3. I_{hERG} decrease and APD increase by long-term exposure to 10 μM 4-HNE

Next, we examined the effect of long-term exposure to 10 μM of 4-HNE (4-HNE_{10L}) on cardiac ion channel currents in GPVMs and HEK293 cells. The cells were divided into two groups; the 4-HNE_{10L} group was pre-incubated with 10 μM 4-HNE in extracellular solution (GPVM) or culture medium (HEK293) for 3 h, and the control group pretreated with an equal amount of solvent (0.015% ethanol). It has to be noted that 4-HNE was not included in the bath perfusate during patch clamp recording. The I_{Kr} and I_{Ks} densities were obtained by digitally subtracting the current sensitive to selective inhibitors, E4031 and Ch293B, respectively (Fig. 4A–D). Neither Ch293B-sensitive I_{Ks} nor $I_{Ca,L}$, was affected by 4-HNE_{10L} (Fig. 4D–F). However, the amplitude of I_{Kr}, i.e. E4031-sensitive current, was significantly reduced by 4-HNE_{10L} (Fig. 4B; peak tail current after 50 mV of activation voltage, 0.66 ± 0.05 and 0.43 ± 0.12 pA/pF for control and 4-HNE, respectively). The APD of 4-HNE_{10L}-treated GPVMs was significnatly longer than that of the control group (Fig. 4G and H; 64%, APD_{90} of 274.6 ± 12.26 and 452.7 ± 28.43 ms for control and 4-HNE_{10L}, respectively). The V_{max}, RMP, and TA of AP were not different between the control and HNE_{10L}-treated groups (Fig. 4H).

In hERG-HEK cells, 4-HNE_{10L} also decreased the I_{hERG} (Fig. 5A, B; 1657.1 ± 128.2 and 545.6 ± 128.5 pA for n = 23 and n = 17 for control and 10 μM 4-HNE, respectively). However, pretreatment with 1 μM 4-HNE for 3 h did not reduce the amplitude of I_{hERG} (Fig. 5A, B). We also tested shorter periods of treatment with 10 μM 4-HNE; 1 h exposure decreased I_{hERG} while 30 min was insufficient to induce significant decrease (Fig. 5C and D, 75.7 ± 4.92, 72.3 ± 7.21, 43.2 ± 5.84, and 31.3 ± 9.62 pA/pF for n = 19, n = 12, n = 10, and n = 15 for control, 30 min, 1 h, and 3 h, respectively).

Interestingly, we found that a reducing agent, tris(2-carboxyethyl) phosphine (TCEP) had different recovery effects on the I_{hERG} decrease by 4-HNE_{100S} and 4-HNE_{10L}. TCEP (1 mM) restored I_{hERG} after 4-HNE_{100S} treatment (Fig. 5E, open triangle, from 30.7 to 55.6 pA/pF, n = 5). By contrast, I_{hERG} inhibition by 4-HNE_{10L} was only slightly reversed by TCEP treatment (Fig. 5F, closed circle, from 30.2 to 39.7 pA/pF, n = 4).

3.4. Decrease of plasma membrane hERG expression by 4-HNE_{10L}

Since the I_{hERG} decay by lower concentration of 4-HNE requires the long-term exposure, we hypothesized that 4-HNE_{10L} condition may affect expression of hERG. Accordingly, we investigated membrane levels of hERG in hERG-HEK cells using Western blot analysis and surface biotinylation. As previously reported [23], the total lysates contained two sizes of hERG: fully glycosylated mature hERG (155 kDa) and core-glycosylated immature hERG (135 kDa). In the surface biotinylation assay, membrane expressed hERG corresponded to the size of mature hERG (Fig. 6A). The treatment of hERG-HEK cells with 10 μM 4-HNE for 3 h, i.e. 4-HNE_{10L}, decreased the membrane expressed hERG and the mature hERG level in total lysate (Fig. 6A). We also analyzed the time-dependent changes of hERG expression with 10 μM 4-HNE; the decrease of mature hERG was not significant at 1 h while became significant from 3 h and up to 12 h (Fig. 6B and C, n = 6). Following the 12 h treatment with 4-HNE, another 12 h of washout incubation with control media could recover the mature hERG level (Fig. 6B and C). The patch clamp study also showed time-dependent slow decrease of I_{hERG} by 10 μM 4-HNE. Interestingly, however, the decrease of I_{hERG} was observed from 1 h, and was not significantly reversed by the 12 h washout protocol (Fig. 6D).

Despite the decrease of mature hERG, the relative levels of immature hERG was not increased (Fig. 6C). Thus, we examined whether inhibition of protein degradation could prevent the effect of 4-HNE_{10L} on the mature hERG expression. Treatment of bortezomib (100 nM), an inhibitor of proteasomal degradation, partly prevented the 4-HNE_{10L}-induced decreases in both membrane and mature hERG (Fig. 7A and C). In contrast, bafilomycin (10 nM), a lysosome inhibitor, did not prevent the 4-HNE-mediated reduction in the plasma membrane-expressed hERG (Fig. 7B, D, surface biotinylation assay). Interestingly, however, the bafilomycin treatment increased the amount of mature hERG in the total lysate irrespective of 4-HNE_{10L} (Fig. 7D, see Discussion 4.3).

Table 1
Modified hERG residues identified after 4-HNE exposure[a].

Peptide	Modified amino acid	Adduct form
SREScASVR	C276	Michael
IGWLHNLGDQIGk	K595	Schiff base
PCTCDFLhGPR	H70	Michael
FhQIPNPLRQR	H687	Michael
cPAPTPSLLNIPLSSPGR[b]	C1015	Michael
THNVTEk[b]	K373	Schiff base
PFRGATk[b]	K748	Schiff base
VARkLDR[b]	K538	Michael

[a] Specific sites of hERG modification by 100 μM 4-HNE identified by ESI LTQ Orbitrap tandem MS/MS with tryptic digests.
[b] Intrinsic modification sites identified from both 4-HNE- and non-treated hERG.

4. Discussion

In the present study, we found multiple sites of irreversible PTM of hERG by 4-HNE, and demonstrated that 4-HNE-mediated inhibition of

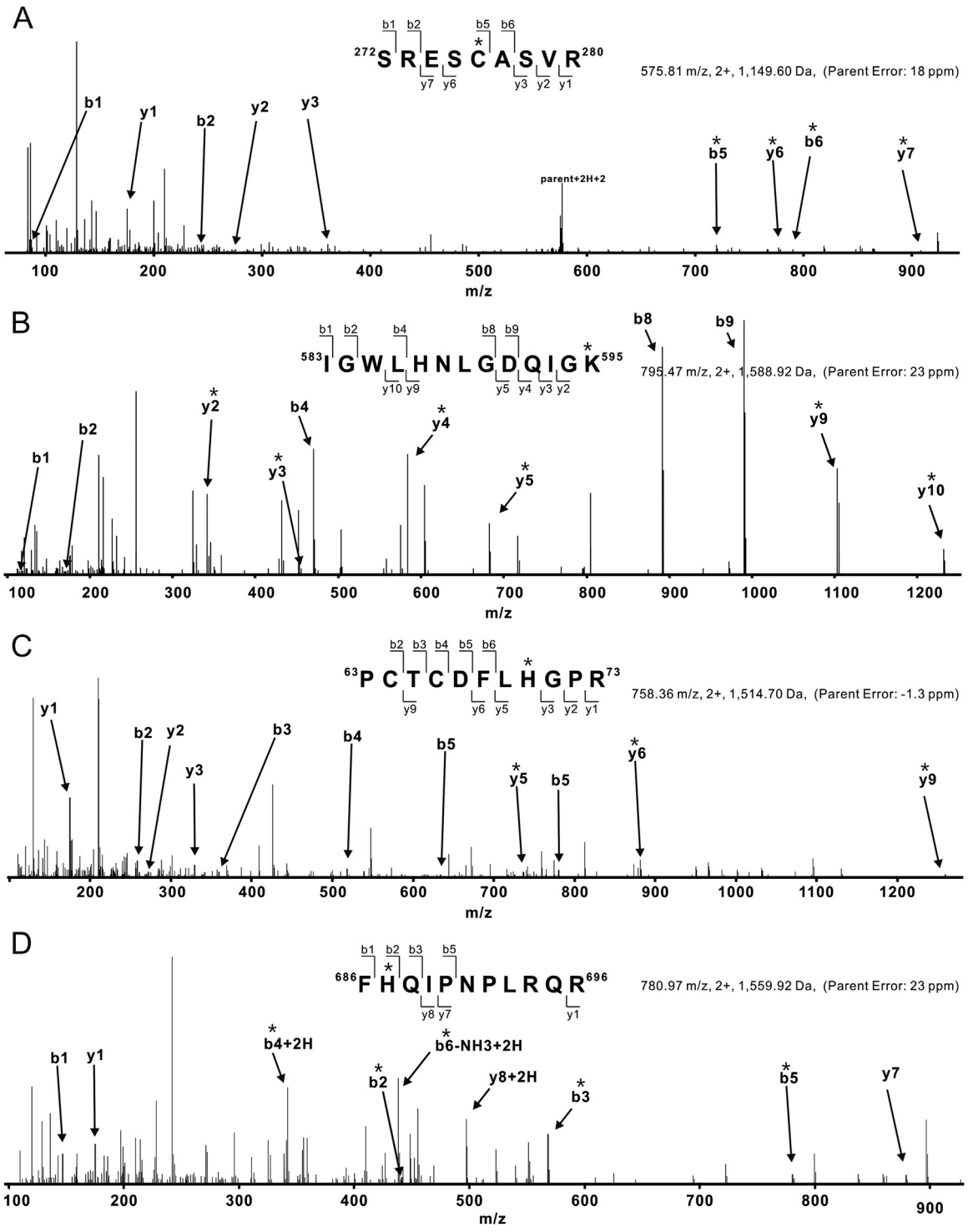

Fig. 3. LC/MS/MS CID mass spectra of 4-HNE-modified hERG peptides. (A-D) Tryptically digested peptides are sufficiently fragmented (SREScASVR, IGWLHNLGDQIGk, PCTCDFLhGPR, and FhQIPNPLRQR, respectively). The sites of the 4-HNE Michael addition (A, C, and D) or Schiff base addition (B) are localized to Cys^{276}, Lys^{595}, His^{70}, and His^{687} by analysis of *b* and *y* ion fragmentation patterns. The product ions containing 4-HNE addition are indicated with asterisks. (A) The mass addition of 156.1 to the *b* and *y* ions containing Cys^{276}, including y_6, y_7, b_5, and b_6, combined with the absence of this addition to y_1–y_3, b_1, and b_2 identifies Cys^{276} as the 4-HNE-modified amino acid. (B) Ions b_1, b_2, b_4, b_8, and b_9 lack the addition of 138.1 that is present on ions y_2–y_5, y_9, and y_{10}. Therefore, localizing the Schiff base adduct to Lys^{595}. (C) Ions y_1–y_3 and b_2–b_6 lack the addition of 156.1 that is present on ions y_5, y_6, and y_9 (His^{70}). (D) Ions y_1, y_7, y_8, and b_1 lack the addition of 156.1 and ions containing His^{687} show the addition (b_2, b_3, and b_5).

hERG along with the prolongation of cardiac APD. Our results suggest that the I_{hERG} inhibition occur through at least two distinct mechanisms. A relatively high concentration (100 μM) of 4-HNE inhibited hERG activity within a few minutes. By contrast, prolonged exposure (> 1 h) to 4-HNE induced the reduction in membrane hERG expression through the retrograde proteasomal degradation, at least partly.

4.1. Physiological implication

Increased levels of 4-HNE as a result of oxidative stress could induce

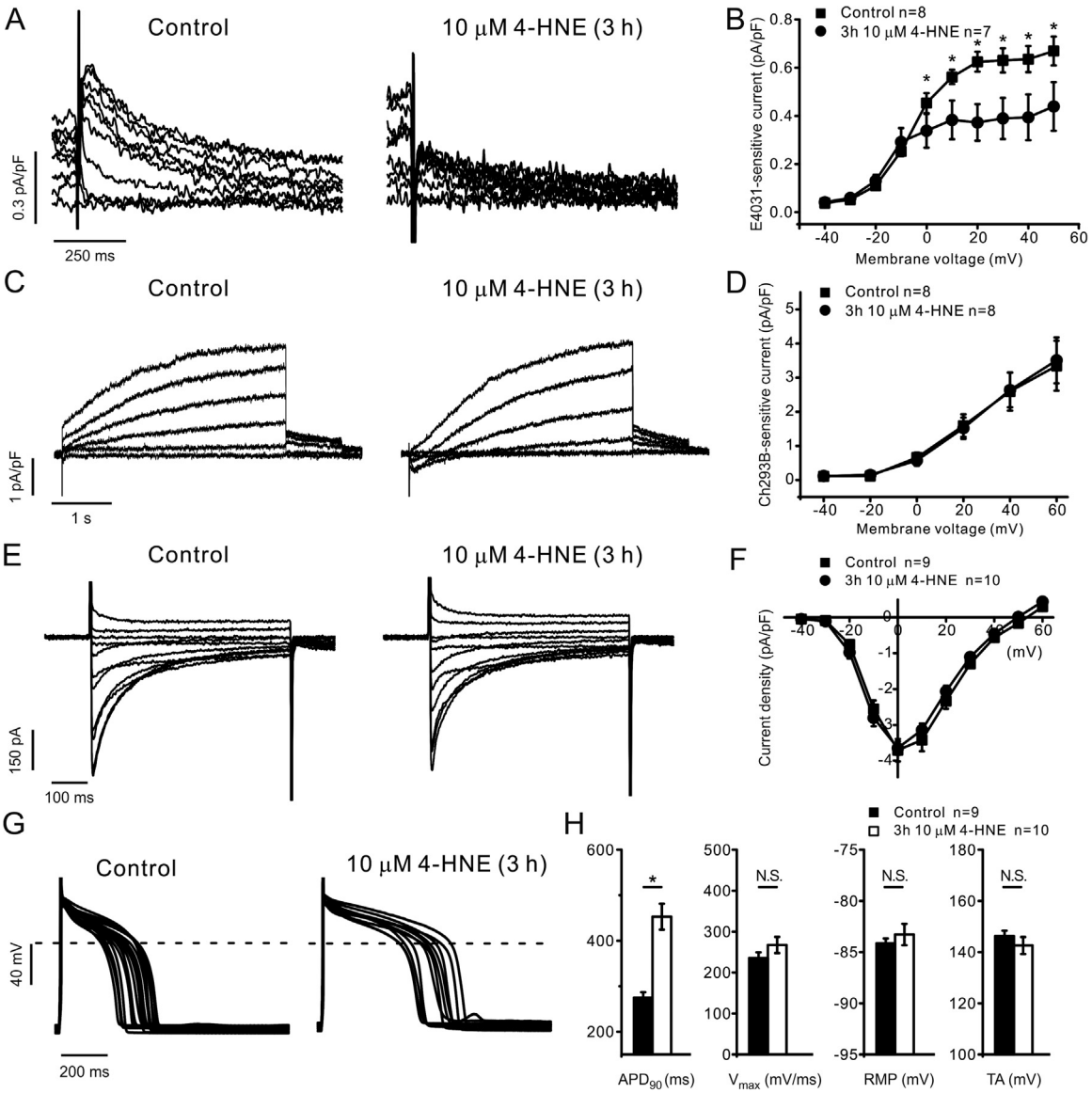

Fig. 4. Effect of 4-HNE$_{10L}$ on the ionic currents and APs of GPVMs. (A–D) I_{Kr} and I_{Ks} were obtained from digital subtraction of the currents sensitive to specific inhibitors; E4031 (1 μM, I_{Kr}) and Ch293B (10 μM, I_{Ks}). I/V curves of I_{Kr} tail currents show significant inhibition by 4-HNE$_{10L}$ (B) while no significant change in I_{Ks} (D). (E, F) $I_{Ca,L}$ amplitudes were not affected by 4-HNE$_{10L}$. (G and H) Overlaid APs from control (n = 9) and 4-HNE$_{10L}$ (n = 10) GPVMs. (H) Summary of the AP parameters showing significant increase of APD_{90} by 4-HNE$_{10L}$.

pathophysiological changes in the heart [18,24,25]. Previous reports have discovered acquired QT prolongation in oxidative stress-related cardiac disease models and patients; patients with acute myocardial ischemia [26], undergoing balloon angioplasty [27], and patients or animal models of doxorubicin-induced cardiotoxicity [28,29]. In fact, treatment with antioxidants was protective in the doxorubicin-induced cardiotoxicity model [30]. It is of interest that a higher prevalence of QT prolongation has been also reported in chronic metabolic disease patients with both type-1 and − 2 diabetes [31]. Considering the critical role of I_{hERG} (I_{Kr}) in cardiac repolarization, we cautiously suggest both acute and chronic inhibition of hERG by 4-HNE may partly contribute to the increased proarrhythmic risk in oxidative stress-related diseases.

4.2. Acute inhibition of I_{hERG} by 4-HNE

The present electrophysiological study suggest that the inhibitory effect of 4-HNE$_{100S}$ reflects functional inhibition of hERG activity. Formation of 4-HNE adducts, a form of oxidative modification of proteins, could influence protein function and expression [32,33]. Although the 4-HNE adduct formation might also modulate ion channels, direct investigation with electrophysiological analysis is relatively rare. A representative case is TRPA1 cation channels activated by reactive oxygen/nitrogen species and electrophilic compounds including 4-HNE. The acute activation of TRPA1 by electrophilic compound is reportedly mediated through four cysteine residues in the cytoplasmic N-terminus [34,35]. In TRPV1, the representative thermo- and chemo-sensitive vanilloid type TRP channel protein, the activation by capsaicin was inhibited by 4-HNE where the adduct formation involving Cys^{621} in the pore region was suggested as the mechanism [36,37].

In hERG channels, a previous study has identified that Cys^{723} in the cytoplasmic C-terminal is responsible for the oxidative inhibition by H_2O_2 [6]. Although our results of LC MS/MS experiment revealed the formation of multiple PTM sites by 4-HNE$_{100S}$ in hERG; Cys^{276}, Lys^{595}, His^{70}, and His^{687} (Table 1 and Fig. 3). Cys^{723} was not found to be modified by 10 min exposure to 100 μM 4-HNE. Furthermore, a preliminary study showed that the Ala substitution of Cys^{723} did not affect the inhibition of I_{hERG} by 4-HNE$_{100S}$ (data not shown). Although we

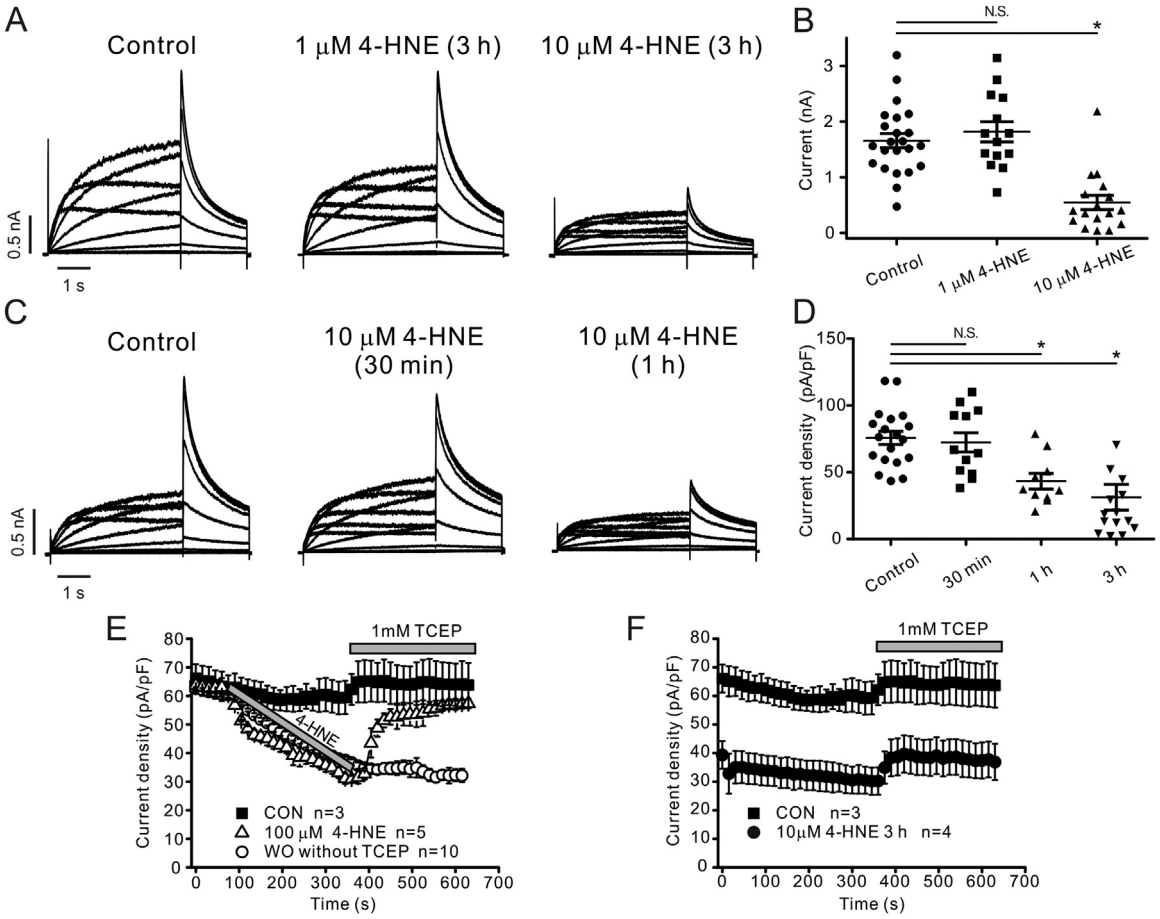

Fig. 5. Concentration- and time-dependent I_{hERG} inhibition by long-term exposure of hERG-HEK cells to 4-HNE. (A, B) The 3 h pre-incubation with 10 μM, but not 1 μM, 4-HNE reduced the amplitude of I_{hERG}. (C, D) Suppression of I_{hERG} was observed after both a 1 and 3 h, but not 30 min, pre-incubation with 10 μM 4-HNE. (B, D) For each group, the peak amplitudes or densities of outward tail current induced by 50 mV of test pulse were plotted with different symbols. (E, F) Differential effects of reducing agents, TCEP (1 mM) on the I_{hERG} inhibition by 4-HNE_{100S} and by 4-HNE_{10L}. Summary of peak tail currents were plotted against the time of experiment. The TCEP treatment alone slightly increased I_{hERG} of both control and 4-HNE_{10L} groups. By contrast, the I_{hERG} reduced by 4-HNE_{100S} was significantly restored by TCEP (open triangle, from 30.7 to 55.6 pA/pF, n = 5). The control data are same in E and F. All data were analyzed with unpaired *t*-tests, where a $P < 0.05$ was considered statistically significant.

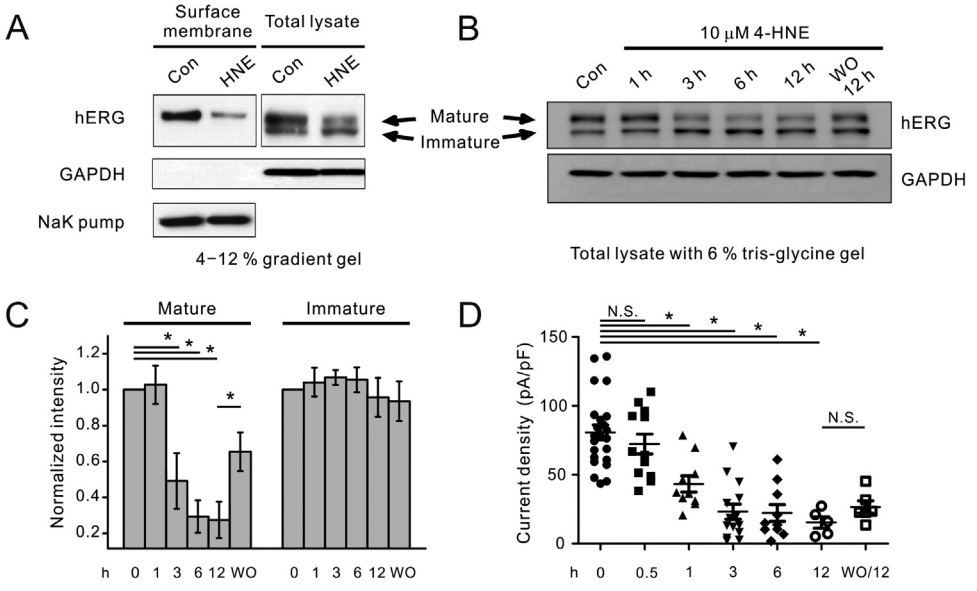

Fig. 6. Effect of 4-HNE_{10L} on hERG protein expression. (A) hERG protein levels in the plasma membrane were measured by surface biotinylation. Western blot analysis of hERG in total lysate revealed both mature (glycosylated higher molecular weight) and immature forms. 4-HNE_{10L} decreased membrane hERG expression along with the mature hERG level. (B and C) Mature hERG expression, but not the levels of immature form, was time-dependently decreased by 4-HNE_{10L} (n = 6). The reduction of mature hERG was partly recovered at 12 h after washout (WO, 12 h). To separate mature and immature hERG bands more clearly, total cell lysates were run on 6% tris-glycine gels. (D) Analysis of I_{hERG} densities during the long-term 4-HNE. Peak amplitudes of I_{hERG} tail currents were plotted at each time points of exposure to 10 μM 4-HNE. Significant decrease was distinguishable from 1 h. Different from the recovery of mature hERG expression, the reduced I_{hERG} was not significantly reversed by 12 h WO (15.3 ± 4.15 and 26.6 ± 4.41 pA/pF for 12 h 4-HNE and WO/12, respectively; P = 0.37). All data were analyzed using unpaired *t*-tests, where a $P < 0.05$ was considered statistically significant.

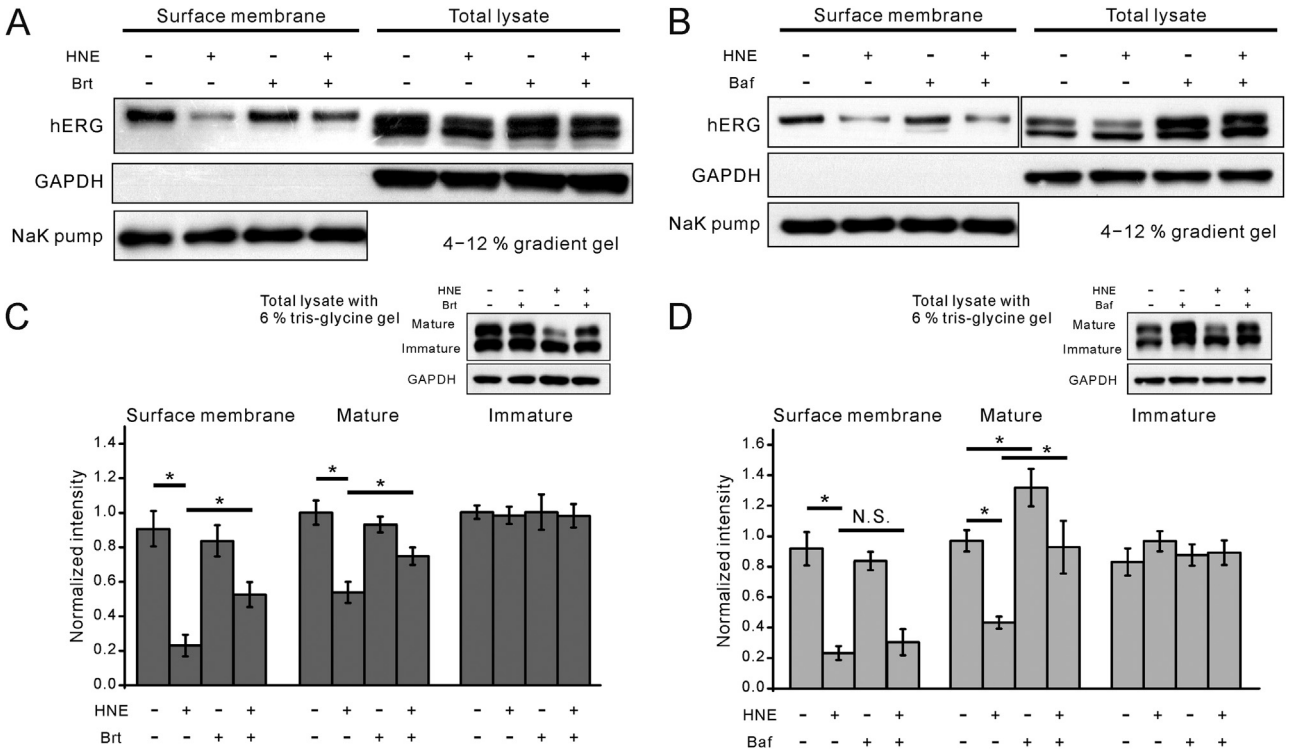

Fig. 7. Effects of proteasomal and lysosomal degradation inhibitors on hERG expression. (A and C) Co-application of proteosomal inhibitor (bortezomib,100 nM) with 4-HNE prevented the 4-HNE_{10L}-induced reduction in membrane expressed hERG (surface biotinylation) and mature form hERG (Total lysate, n = 7). (B and D) Treatment with the lysosome inhibitor, 10 nM bafilomycin, did not prevent the reduction of surface hERG by 4-HNE_{10L}. The increases of mature form hERG by bafilomycin co-treatment were observed irrespective of 4-HNE treatment (n = 6). To further separate mature and immature hERG bands, total cell lysates were also run on 6% tris-glycine gels. All data were analyzed using unpaired *t*-tests, where $P < 0.05$ was considered statistically significant.

found the four candidate sites (Cys^{276}, Lys^{595}, His^{70}, and His^{687}), we did not rigorously investigate all the possible combinations of site-directed mutagenesis of hERG yet. Future investigations would be necessary to correlate the specific PTM location with the changes of I_{hERG}. The recovery of acutely suppressed I_{hERG} by TCEP treatment was quite interesting while somewhat difficult to explain. Since the conjugate bonding formation like 4-HNE adduct would not be easily reversed by simple reducing agent, the mechanism of I_{hERG} recovery by TCEP might not simply explained by chemical reducing effects, which also requires future investigation.

4.3. Slow downregulation of mature hERG by 4-HNE

Western blot analysis and surface biotinylation assay indicate the downregulation of the mature form of hERG in plasma membrane underlies the irreversible inhibition of I_{hERG} by 4-HNE_{10L}. Furthermore, the restoration of mature hERG expression along with I_{hERG} by bortezomib implicate ubiquitination-dependent degradation of membrane hERG under long-term exposure (> 1 h) to 4-HNE.

There have been studies that have identified the mechanisms of hERG suppression as the facilitated internalization and degradation of membrane hERG through monoubiquitination-dependent proteasomal or lysosomal degradation. Treatment with the lipid molecule ceramide or antidepressant desipramine could reduce mature hERG expression via the ubiquitination-dependent lysosomal degradation pathway, resulting in drug-induced long QT syndrome [38,39]. Also, it has been reported that chronic conditioning with low extracellular K^+ also causes hERG internalization and degradation through the caveolin and ubiquitination pathways, which can be inhibited by proteasome and lysosome inhibitors [40,41].

Previous studies have shown the lysosomal inhibitor bafilomycin alone does not affect hERG protein levels under physiological state [39,40]. We also investigated the effects of bafilomycin, and found that the relative extent of mature hERG reduction by 4-HNE_{10L} was partly alleviated. However, the application of bafilomycin alone significantly increased the levels of mature hERG, irrespective of 4-HNE_{10L} (Fig. 7B and D). Furthermore, since the surface biotinylation assay did not show the preventive effects of bafilomycin (Fig. 7B, D), it is unlikely that the lysosomal pathway is responsible for the surface hERG downregulation by 4-HNE_{10L}.

Recently, Lamothe et al. reported that prolonged hypoxia of neonatal rat ventricular myocytes (0.5% O_2, > 6 h) causes a marked reduction in mature hERG channels and prolongs the APD through upregulation of the protease calpain [42]. The calpain-dependent degradation pathway has also been suggested to be involved in 4-HNE-induced disruption of gap junctions in cochlear spiral ligaments [43]. In this respect, in addition to proteasomal/lysosomal degradation, upregulation of protease may be a possible yet-to-be investigated mechanism of hERG suppression by 4-HNE_{10L}.

5. Conclusion

Our study demonstrates 4-HNE has multiple inhibitory effects on cardiac ion channels. Of these, functional downregulation of hERG was associated with prolongation of APD. We propose at least two mechanisms accounted for hERG inhibition by 4-HNE: 1) direct PTM on 4 different hERG residues and 2) degradation of membrane hERG. We cautiously suggest that 4-HNE-mediated hERG inhibition might partly underlie the arrhythmogenic risk through APD prolongation under oxidative stress.

Acknowledgements

This work was supported by the Cooperative Research Program of

Basic Medical Science and Clinical Science from Seoul National University College of Medicine (800-20170157), and by EDISON Research Program and Basic Science Research Program through the National Research Foundation of Korea (NRF) funded by the Korean Government, Ministry of Education (NRF-2016M3C1A6936605) and Ministry of Science and ICT (NRF-2016R1D1A1A02937499), and by the Research Center for High Quality Livestock Products through Agriculture, funded by the Korean Government, Ministry of Agriculture, Food and Rural Affairs (715003-07).

Conflicts of interest

The authors state no conflict of interest.

References

[1] M.C. Sanguinetti, M. Tristani-Firouzi, hERG potassium channels and cardiac arrhythmia, Nature 440 (7083) (2006) 463–469.
[2] J.I. Vandenberg, M.D. Perry, M.J. Perrin, S.A. Mann, Y. Ke, A.P. Hill, hERG K^+ channels: structure, function, and clinical significance, Physiol. Rev. 92 (3) (2012) 1393–1478.
[3] J. Nanduri, N. Wang, P. Bergson, N.R. Prabhakar, et al., Mitochondrial reactive oxygen species mediate hypoxic down-regulation of hERG channel protein, Biochem. Biophys. Res. Commun. 373 (2) (2008) 309–314.
[4] M. Taglialatela, P. Castaldo, S. Iossa, et al., Regulation of the human ether-a-gogo related gene (HERG) K^+ channels by reactive oxygen species, Proc. Natl. Acad. Sci. USA 94 (21) (1997) 11698–11703.
[5] J. Wang, H. Wang, Y. Zhang, et al., Impairment of HERG K^+ channel function by tumor necrosis factor-alpha: role of reactive oxygen species as a mediator, J. Biol. Chem. 279 (14) (2004) 13289–13292.
[6] K. Kolbe, R. Schonherr, G. Gessner, et al., Cysteine 723 in the C-linker segment confers oxidative inhibition of hERG1 potassium channels, J. Physiol. 558 (2010) 2999–3009.
[7] W. Siems, T. Grune, Intracellular metabolism of 4-hydroxynonenal, Mol. Asp. Med. 24 (4–5) (2003) 167–175.
[8] C.M. Spickett, The lipid peroxidation product 4-hydroxy-2-nonenal: advances in chemistry and analysis, Redox Biol. 1 (2013) 145–152.
[9] M. Csala, T. Kardon, B. Legeza, et al., On the role of 4-hydroxynonenal in health and disease, Biochim. Biophys. Acta 1852 (5) (2015) 826–838.
[10] M. Mol, L. Regazzoni, A. Altomare, et al., Enzymatic and non-enzymatic detoxification of 4-hydroxynonenal: methodological aspects and biological consequences, Free Radic. Biol. Med. 111 (2017) 328–344.
[11] J.P. Castro, T. Jung, T. Grune, W. Siems, 4-Hydroxynonenal (HNE) modified proteins in metabolic diseases, Free Radic. Biol. Med. 111 (2017) 309–315.
[12] H. Esterbauer, R.J. Schaur, H. Zollner, Chemistry and biochemistry of 4-hydroxynonenal, malonaldehyde and related aldehydes, Free Radic. Biol. Med. 11 (1) (1991) 81–128.
[13] H. Zhang, H.J. Forman, 4-hydroxynonenal-mediated signaling and aging, Free Radic. Biol. Med. 111 (2017) 219–225.
[14] J.M. Guo, A.J. Liu, P. Zang, et al., ALDH2 protects against stroke by clearing 4-HNE, Cell Res. 23 (7) (2013) 915–930.
[15] W.C. Lee, H.Y. Wong, Y.Y. Chai, et al., Lipid peroxidation dysregulation in ischemic stroke: plasma 4-HNE as a potential biomarker? Biochem. Biophys. Res. Commun. 425 (4) (2012) 842–847.
[16] C. Asselin, Y. Shi, R. Clement, J.C. Tardif, C. Des Rosiers, Higher circulating 4-hydroxynonenal-protein thioether adducts correlate with more severe diastolic dysfunction in spontaneously hypertensive rats, Redox Rep. 12 (1) (2007) 68–72.
[17] V. Calabrese, C. Mancuso, M. Sapienza, et al., Oxidative stress and cellular stress response in diabetic nephropathy, Cell Stress Chaperon. 12 (4) (2007) 299–306.
[18] P. Eaton, J.M. Li, D.J. Hearse, M.J. Shattock, Formation of 4-hydroxy-2-nonenal-modified proteins in ischemic rat heart, Am. J. Physiol. 276 (3) (1999) H935–H943.
[19] G. Leonarduzzi, E. Chiarpotto, F. Biasi, G. Poli, 4-Hydroxynonenal and cholesterol oxidation products in atherosclerosis, Mol. Nutr. Food Res. 49 (11) (2005) 1044–1049.
[20] A. Bhatnagar, Electrophysiological effects of 4-hydroxynonenal, an aldehydic product of lipid peroxidation, on isolated rat ventricular myocytes, Circ. Res. 76 (2) (1995) 293–304.
[21] S.W. Choi, K.S. Kim, D.H. Shin, et al., Class 3 inhibition of hERG K^+ channel by caffeic acid phenethyl ester (CAPE) and curcumin, Pflüg. Arch. - Eur. J. Physiol. 465 (8) (2013) 1121–1134.
[22] J.M. Berman, M.S. Awayda, Redox artifacts in electrophysiological recordings, Am. J. Physiol. Cell Physiol. 304 (7) (2013) C604–C613.
[23] Q. Gong, C.L. Anderson, C.T. January, Z. Zhou, Role of glycosylation in cell surface expression and stability of HERG potassium channels, Am. J. Physiol. Heart Circ. Physiol. 283 (1) (2002) H77–H84.
[24] M.P. Mattson, Roles of the lipid peroxidation product 4-hydroxynonenal in obesity, the metabolic syndrome, and associated vascular and neurodegenerative disorders, Exp. Gerontol. 44 (10) (2009) 625–633.
[25] A. Sun, Y. Cheng, Y. Zhang, et al., Aldehyde dehydrogenase 2 ameliorates doxorubicin-induced myocardial dysfunction through detoxification of 4-HNE and suppression of autophagy, J. Mol. Cell. Cardiol. 71 (2014) 92–104.
[26] M. Bijl, F.W. Verheugt, Extreme QT prolongation solely due to reversible myocardial ischemia in single-vessel coronary disease, Am. Heart J. 123 (2) (1992) 524–526.
[27] D.N. Kenigsberg, S. Khanal, M. Kowalski, S.C. Krishnan, Prolongation of the QTc interval is seen uniformly during early transmural ischemia, J. Am. Coll. Cardiol. 49 (12) (2007) 1299–1305.
[28] J. Ducroq, H. Moha ou Maati, S. Guilbot, et al., Dexrazoxane protects the heart from acute doxorubicin-induced QT prolongation: a key role for I(Ks), Br. J. Pharmacol. 159 (1) (2010) 93–101.
[29] S. Kharin, V. Krandycheva, A. Tsvetkova, M. Strelkova, D. Shmakov, Remodeling of ventricular repolarization in a chronic doxorubicin cardiotoxicity rat model, Fundam. Clin. Pharmacol. 27 (4) (2013) 364–372.
[30] Y. Xin, S. Zhang, L. Gu, et al., Electrocardiographic and biochemical evidence for the cardioprotective effect of antioxidants in acute doxorubicin-induced cardiotoxicity in the beagle dogs, Biol. Pharm. Bull. 34 (10) (2011) 1523–1526.
[31] Z. Lu, L. Lense, M. Sharma, et al., Prevalence of QT prolongation and associated LVEF changes in diabetic patients over a four-year retrospective time period, J. Commun. Hosp. Intern. Med. Perspect. 7 (2) (2017) 87–94.
[32] A. Ayala, M.F. Munoz, S. Arguelles, Lipid peroxidation: production, metabolism, and signaling mechanisms of malondialdehyde and 4-hydroxy-2-nonenal, Oxid. Med. Cell. Longev. 2014 (2014) 360438.
[33] S. Dalleau, M. Baradat, F. Gueraud, L. Huc, Cell death and diseases related to oxidative stress: 4-hydroxynonenal (HNE) in the balance, Cell Death Differ. 20 (12) (2013) 1615–1630.
[34] M. Trevisani, J. Siemens, S. Materazzi, et al., 4-Hydroxynonenal, an endogenous aldehyde, causes pain and neurogenic inflammation through activation of the irritant receptor TRPA1, Proc. Natl. Acad. Sci. USA 104 (33) (2007) 13519–13524.
[35] D. Kozai, N. Ogawa, Y. Mori, Redox regulation of transient receptor potential channels, Antioxid. Redox Signal. 21 (6) (2014) 971–986.
[36] D.J. DelloStritto, P. Sinharoy, P.J. Connell, et al., 4-Hydroxynonenal dependent alteration of TRPV1-mediated coronary microvascular signaling, Free Radic. Biol. Med. 101 (2016) 10–19.
[37] Y. Jin, D.K. Kim, L.Y. Khil, et al., Thimerosal decreases TRPV1 activity by oxidation of extracellular sulfhydryl residues, Neurosci. Lett. 369 (3) (2004) 250–255.
[38] H. Chapman, C. Ramstrom, L. Korhonen, et al., Downregulation of the HERG (KCNH2) K^+ channel by ceramide: evidence for ubiquitin-mediated lysosomal degradation, J. Cell Sci. 118 (Pt 22) (2005) 5325–5334.
[39] A.T. Dennis, D. Nassal, I. Deschenes, D. Thomas, E. Ficker, Antidepressant-induced ubiquitination and degradation of the cardiac potassium channel hERG, J. Biol. Chem. 286 (39) (2011) 34413–34425.
[40] J. Guo, H. Massaeli, J. Xu, et al., Extracellular K^+ concentration controls cell surface density of IKr in rabbit hearts and of the HERG channel in human cell lines, J. Clin. Investig. 119 (9) (2009) 2745–2757.
[41] H. Massaeli, T. Sun, X. Li, et al., Involvement of caveolin in low K^+-induced endocytic degradation of cell-surface human ether-a-go-go-related gene (hERG) channels, J. Biol. Chem. 285 (35) (2010) 27259–27264.
[42] S.M. Lamothe, W. Song, J. Guo, et al., Hypoxia reduces mature hERG channels through calpain up-regulation, Fed. Am. Soc. Exp. Biol. J. 31 (11) (2017) 5068–5077.
[43] T. Yamaguchi, M. Yoneyama, E. Hinoi, K. Ogita, Involvement of calpain in 4-hydroxynonenal-induced disruption of gap junction-mediated intercellular communication among fibrocytes in primary cultures derived from the cochlear spiral ligament, J. Pharmacol. Sci. 129 (2) (2015) 127–134.